BULLETIN OF THE POLISH ACADEMY OF SCIENCES
TECHNICAL SCIENCES,
DOI: 10.24425/bpasts.2026.158774

Dynamic Simulation of a Vacuum Packed Particles Torsional Damper with ABS–NBR Particle Mixtures Using a Modified Bouc–Wen Model

Dominik Rodak [1]*; **Mateusz Żurawski** [1]**; **and Robert Zalewski** [1]***

[1] Warsaw University of Technology, Faulty of Automotive and Construction Machinery Engineering, Narbutta 84, 02-524 Warsaw

Abstract. Vacuum Packed Particles Torsional Dampers (VPPTDs) are adaptive devices capable of providing tunable damping through the adjustment of underpressure inside a granular-filled chamber. Despite their promising applications in vibration control, accurately modeling their highly nonlinear and hysteretic behavior remains a significant challenge. This paper shows a modified Bouc-Wen model that incorporates an additional nonlinear stiffness term and a dry friction component to better represent the torque-angular displacement relationship under varying operational conditions. Quasi-static experiments were conducted on a dedicated test stand with harmonic excitation (±10°) across frequencies from 0.0 to 0.8 Hz and underpressures ranging from 0.00 to 0.09 MPa. Various granular mixtures composed of Acrylonitrile Butadiene Styrene (ABS) and Nitrile Butadiene Rubber (NBR) particles in volume ratios of 1:0, 3:1, 1:1, 1:3, and 0:1 were investigated. The shape and area of the hysteresis loops were found to depend strongly on both the mixture composition and the vacuum level. Model parameters were identified using evolutionary algorithms and expressed as functions of underpressure, allowing the simulation of pressure-dependent damping and stiffness behavior. Dynamic simulations based on the identified models confirmed that adjusting the vacuum level effectively changes the system's dynamic response. The results demonstrate that the proposed model reliably captures the complex hysteretic behavior of VPPTDs and confirms the feasibility of employing underpressure as an effective control variable in adaptive damping applications.

Key words: Vacuum Packed Particles Damper; Adaptive Damping; Bouc-Wen Model; Hysteresis Modeling; Nonlinear Dynamics

1. INTRODUCTION

Vibration damping remains a significant challenge in modern engineering. Traditional structures often rely on passive damping systems, which are effective only under specific conditions. However, there is a growing interest in replacing passive systems with active or semi-active solutions, especially when structures are exposed to varying external excitations.

To address this need, various adaptive vibration damping methods have been developed. These include the use of magnetorheological fluids (MR), piezoelectric materials, and active hydraulic systems. Each of these technologies offers the ability to adjust the mechanical response of a system in real time, improving performance under dynamic conditions [1, 2, 3].

Research on vacuum-based granular and structured media has shown their potential for the development of adaptive mechanical systems with controllable stiffness and damping characteristics. Studies on structured fabrics formed by interlocking particles enclosed in vacuum bags demonstrated that the application of negative pressure leads to a jamming transition, which increases the bending stiffness of the structure while the system remains highly flexible in the unjammed state. Both experimental investigations and numerical simulations of chain-mail-type assemblies indicated that the macroscopic mechanical response is strongly affected by particle geometry, contact interactions and interlocking mechanisms, which determine the transition between compliant and stiff configurations. Later studies examined the dynamic behavior of vacuum-packed structured fabrics and showed that the stiffness and natural frequencies of beam-like elements can be adjusted by changing the vacuum level, making it possible to design adaptive vibration absorbers. These works also indicated that the dynamic response depends not only on the vacuum pressure but also on the particle topology, the number of fabric layers and friction between neighboring particles. However, most existing studies have considered systems composed of a single type of particle and structured chain-mail geometries [4, 5, 6].

One particularly promising technology in this area is the use of Vacuum-Packed Particles (VPP). The VPP structures consist of granular materials enclosed in a flexible envelope. When vacuum is applied inside the envelope, it compresses around the particles, increasing the contact forces between them. This leads to higher friction, deformation of the particles, and causes difficulties in granular core reorganisation [7, 8, 9, 10, 11].

The VPP structures exhibit hysteretic behaviour that depends on several factors, such as the type and shape of the granules or the shape of the structure, but most importantly, their mechanical properties can be controlled in real time by adjusting the internal vacuum level. This makes VPP an attractive option for adaptive damping applications.

A notable example of a VPP application is the VPP Torsional Damper (VPPTD), which is described in detail in [12, 13]. This device demonstrates how VPP structures can be used effectively to damp torsional vibrations, further highlighting their potential in engineering design.

*e-mail: Dominik.Rodak@pw.edu.pl
**e-mail: Mateusz.Żurawski@pw.edu.pl
***e-mail: Robert.Zalewski@pw.edu.pl

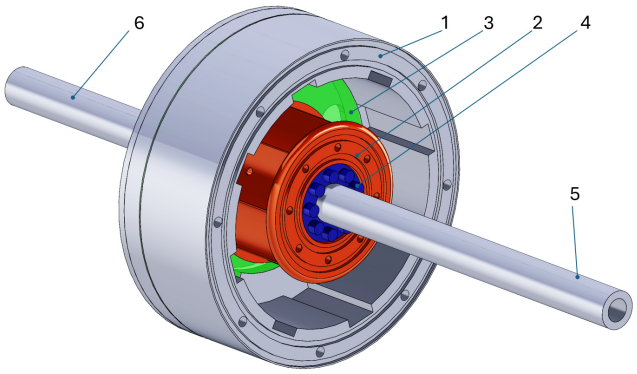

Fig. 1. Scheme of VPP TD

1.1. VPPTD

The VPP Torsional Damper (VPPTD), shown in Figure 1, consists of a working chamber built from an outer ring (1), an inner ring (2) and two membranes (3) made of silicone film. The chamber is filled with granular material. The drive shaft (6) is connected to the outer ring, while the driven shaft (5) is connected to the inner ring by a clamping sleeve (4).

Air is evacuated from the chamber through the inner ring and the driven shaft, which is hollow. This allows for vacuum control inside the VPP structure. The outer and inner rings are able to move relative to each other, which enables torsional motion to be transmitted through the granular core.

By adjusting the vacuum level, the mechanical properties of the damper can be changed in real time, allowing for adaptive control of torsional damping depending on operating conditions. The mechanical characteristics of the VPP Torsional Damper (VPPTD) exhibit clear symmetric hysteresis. Moreover, the VPPTD shows rate-independent behaviour, which means that its response does not significantly depend on the speed of deformation.

Modelling hysteresis loops is a challenge in itself, and many rate-independent hysteresis models have been proposed in the literature. Notable examples include the Preisach model, the Bouc-Wen model, the Dahl model, and the Vaiana model [14, 15, 16, 17, 18, 19].

In the study presented in [12], the authors used a modified Bouc-Wen model, enhanced with terms for non-linear stiffness and dry friction. The model parameters were identified on the basis of quasi-static torsion tests. In addition, functions that describe how these parameters vary with vacuum level were determined. These experiments were conducted with ABS material.

The aim of this paper is to perform numerical simulations of a system equipped with a VPPTD under varying vacuum conditions. In addition, simulations were performed for other materials, which are different ratio mixtures of ABS and NBR rubber grains, with model parameters identified in a way similar to the procedure described in [12].

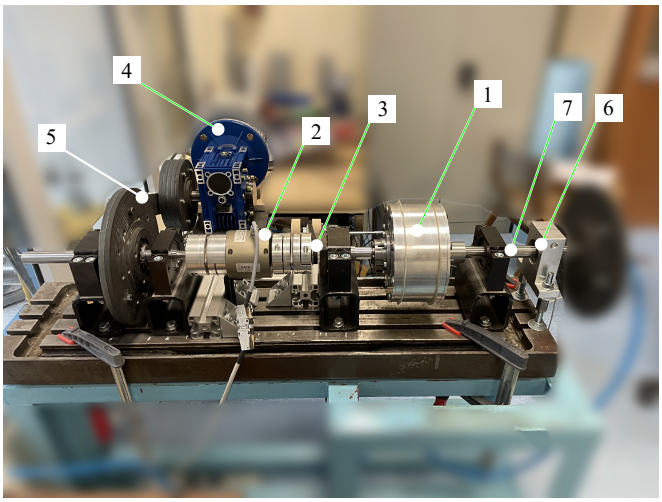

Fig. 2. Test stand [12]

2. TEST STAND

The test stand shown in Figure 2 allows the damper (1) to be driven at various frequencies. A four-bar linkage mechanism (5) driven by an electric motor (4) was used to generate a simple harmonic motion.

The amplitude of the excitation depends on the length of the components of the mechanism and can be adjusted in discrete steps. A torque metre (2) is responsible for measuring the torque, while the angle of rotation is measured using a rotary encoder (3). The driven shaft (7) is fixed and prevented from rotating by a clamping sleeve mounted in (6). The underpressure is applied by a laboratory pump. Pressure measurement is performed using a pressure sensor connected to the working chamber.

The tests were carried out for five different materials, which were mixtures of ABS and NBR granules in various proportions. The mixtures tested were as follows: ABS, ABS-NBR, and NBR in volumetric ratios: $100\% - 0,75\%/25\%, 50\%/50\%, 25\%/75\%$ and $0 - 100\%$, respectively. The grains had a random shape and a characteristic dimension around 3 mm. The chamber fill factor (ratio between the volume of particles and the volume of the chamber) was approximately 0.7 in each case. Each material that fills the VPPTD damper was tested in a vacuum pressure range of 0.00 MPa (atmospheric pressure) to 0.09 MPa in steps of 0.01 MPa and for a frequency range of 0.1 Hz to 0.8 Hz in steps of 0.1 Hz and the th amplitude $\pm 10°$.

Figures 3a - 3e depict the experimental results for each test conducted for the excitation frequency equal to $f = 0.79$ Hz and for various levels of pressure.

3. MODELLING AND IDENTIFICATION

Hysteretic systems with friction can be modelled in many different ways. Among the most well-known approaches are the Bouc-Wen model, the Dahl model, the Preisach model, and the Vaiana model. Each of these models has its own strengths and limitations, depending on the application and the type of hysteresis being described.

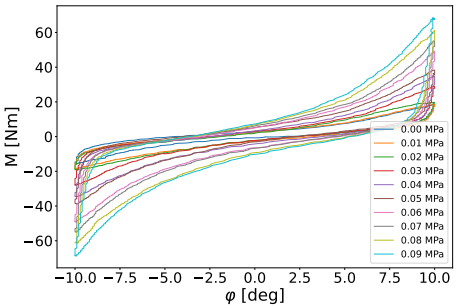

(a) ABS

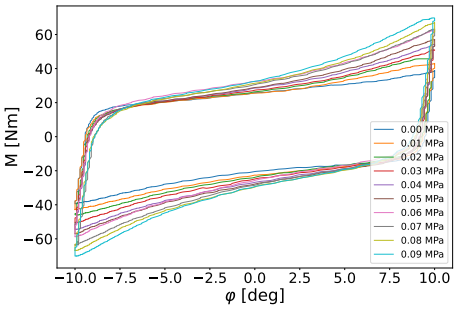

(b) ABS - NBR 3-1

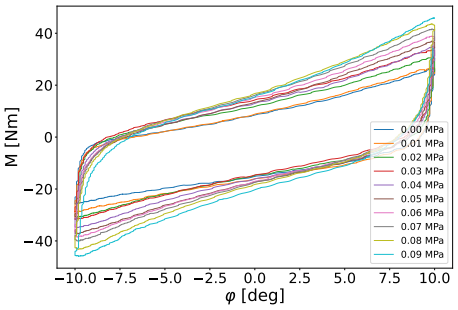

(c) ABS - NBR 1-1

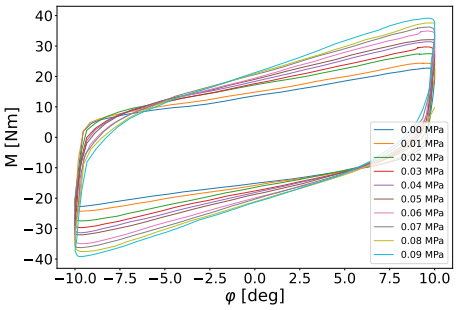

(d) ABS - NBR 1-3

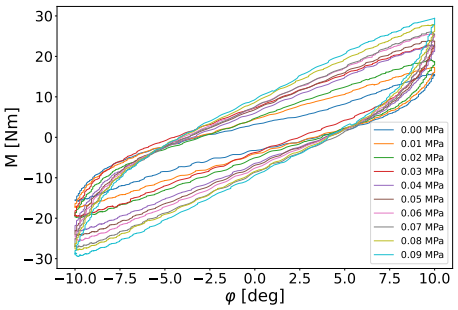

(e) NBR

Fig. 3. Experimental results for various mixtures.

ABS	ABS-NBR 3:1
$D = 12.726p + 2.5581$	$D = 12.602p + 3.1847$
$A = 10.227p + 4.5122$	$A = -7.0758p + 5.0437$
$\beta = 252.3p + 6.9041$	$\beta = 16.705p + 4.3327$
$\gamma = -14.776p - 3$	$\gamma = -27.079p + 0.6223$
$n = 16.356p + 1.0685$	$n = 15.76p + 2.7561$
$c = -8.6701p^2 - 1.549p - 0.0033$	$c = 1.0048p + 0.005$
$\alpha = -479.08p^3 + 106.76p^2 - 7.7916p + 0.5325$	$\alpha = 1.4578p + 0.2421$
$k = 56.164p + 0.7932$	$k = -5.5556p + 4.1$
$k_1 = 0.7068p + 0.0135$	$k_1 = 0.6425p + 0.0247$
$M_s = 109.45p + 2.1562$	$M_s = 55.556p + 13$
ABS-NBR 1:1	**ABS-NBR 1:3**
$D = -16.879p + 4.4261$	$D = -2.174p + 2.72$
$A = -1.4573p + 4.6602$	$A = -3.42p + 4.23$
$\beta = -66.521p + 15.223$	$\beta = -102.96p + 22.33$
$\gamma = -11.9p - 2.6961$	$\gamma = -19.12p - 0.244$
$n = 4.2585p + 1.7688$	$n = 1.433p + 1.8123$
$c = -0.2528p + 0.0546$	$c = -9.86p^2 + 1.49p + 0.028$
$\alpha = 0.187p + 0.289$	$\alpha = 1.916p + 0.1442$
$k = 29.745p + 4.023$	$k = 0.33p + 4.15$
$k_1 = 0.20717p + 0.0092$	$k_1 = 0.15p + 0.0391$
$M_s = 54.896p + 1.792$	$M_s = 35p + 0.9$
NBR	
$D = -4.385p + 1.9212$	
$A = -4.3383p + 3.1217$	
$\beta = -177.48p + 26.669$	
$\gamma = -26.345p - 0.755$	
$n = 1.2294p + 1.6474$	
$c = -12.86p^2 + 2.59p + 0.036$	
$\alpha = 2.9748p + 0.24$	
$k = -7.2219p + 3.7685$	
$k_1 = -0.0317p + 0.0203$	
$M_s = 15.9p + 0.1743$	

Table 1. Parameter functions

The Bouc-Wen model is particularly popular due to its flexibility and relatively simple mathematical structure. One of its main advantages is that it can capture a wide range of hysteresis shapes with a moderate number of parameters. It is also relatively easy to implement numerically, making it a common choice in engineering applications. However, it is a phenomenological model, not a physical one. This means that the parameters of the Bouc-Wen model do not directly correspond to physical properties of the system, such as stiffness or damping. Instead, they represent abstract quantities that need to be calibrated experimentally [20].

Despite its versatility, the standard Bouc-Wen model was not sufficient to accurately represent the behaviour of certain samples, especially those made of ABS or with a high ABS content. These materials exhibit a pinching effect in their hysteresis loops, characterised by a narrowing of the loop near the origin and rapidly increasing slopes at the end of the hysteresis loops. That effects are observed in systems with complex internal friction and energy dissipation mechanisms. Unfortunately, the basic Bouc-Wen formulation cannot capture this behaviour well, leading to poor fitting results for these types of materials.

To address this limitation, a modified version of the Bouc-Wen model was proposed. It includes two additional elements: a nonlinear stiffness term (k_1x^3) to capture geometric or material nonlinearities, and a dry friction component ($M_s \cdot sgn(v)$) to model Coulomb friction effects. These enhancements allow the model to better replicate the observed pinching behaviour and to more accurately reflect the energy dissipation characteristics of the VPPTD. This enhanced model is given by the equations 1 and 2 and is described in detail in [12].

$$I\ddot{\varphi} + c(p)\dot{\varphi} + \alpha(p)\left(k(p)\varphi + k_1(p)\varphi^3\right) + \\ + (1-\alpha(p))D(p)k(p)z + M_s(p)\,\mathrm{sgn}(\dot{\varphi}) = 0 \quad (1)$$

$$\dot{z} = D(p)^{-1}\left(A(p)\dot{\varphi} - \beta(p)|\dot{\varphi}||z|^{n(p)-1}z - \gamma(p)\dot{\varphi}|z|^{n(p)}\right) \quad (2)$$

The proposed model contains 12 parameters. These parameters define the shape, size, and nature of the hysteresis loop. The parameter identification process was carried out using genetic algorithms, which are well suited to exploring complex multidimensional parameter spaces. Genetic algorithms use mechanisms inspired by biological evolution, such as selection, crossover, and mutation, to iteratively improve the fit of the model to the experimental data. The range and relationships between parameters were defined on the basis of the reference work [20], which provides a theoretical foundation for the behaviour of systems with rate-independent hysteresis. With the power of modern computing, even such complex identification tasks can be performed efficiently using stochastic optimisation techniques.

After identification, the following parameter functions depended on the underpressure level inside the damper were obtained and are shown in Table 1. These functions describe how each of the ten model parameters changes as a function of internal pressure, which is crucial for capturing the adaptive nature of the VPPTD.

The fact that model parameters follow well-defined functions of vacuum level (e.g., linear, polynomial, or exponential) suggests that it may be possible to estimate the damper's behaviour across the entire vacuum range by conducting only a few experiments at selected vacuum levels. This opens the door to efficient design and control strategies based on predictive modelling.

4. NUMERICAL SIMULATIONS

Numerical simulations were performed on the basis of the model shown in Figure 4.

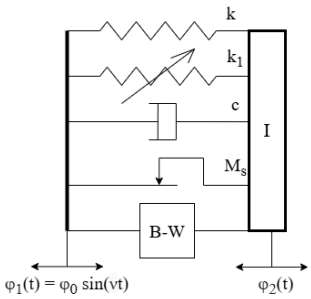

Fig. 4. Scheme of model considerd

The system was kinematically excited using a periodic function defined as 3:

$$\varphi_1(t) = \varphi_0 sin(\nu t) \quad (3)$$

where φ_0 [deg] and ν [rad/s] are the amplitude and frequency of excitation, respectively. The governing equations of the model are presented in equations 4 and 5.

$$I\ddot{\varphi} + c(p)(\dot{\varphi}_2 - \dot{\varphi}_1) + \\ + \alpha(p)\left(k(p)(\varphi_2 - \varphi_1) + k_1(p)(\varphi_2 - \varphi_1)^3\right) + \\ + (1-\alpha(p))D(p)k(p)z + \\ + M_s(p)\,\mathrm{sgn}(\dot{\varphi}_2 - \dot{\varphi}_1) = 0 \quad (4)$$

$$\dot{z} = D(p)^{-1}(A(p)(\dot{\varphi}_2 - \dot{\varphi}_1) - \beta(p)|\dot{\varphi}_2 - \dot{\varphi}_1||z|^{n(p)-1}z + \\ - \gamma(p)(\dot{\varphi}_2 - \dot{\varphi}_1)|z|^{n(p)}) \quad (5)$$

Similarly to the experiments, simulations were performed for each material configuration and for a range of underpressures of 0.01 MPa to 0.09 MPa.

In the first step, free vibration simulations were performed by applying nonzero initial conditions. In this case, the internal variables $\varphi_1(t) = 0$ and $\dot{\varphi}_1(t) = 0$ were set to zero, while the initial rotation and angular velocity of the main mass was nonzero. The initial conditions were selected individually for each material to ensure that at least three oscillation cycles were clearly observable in the time response. Based on these simulations, phase portraits were generated to illustrate the dynamic behaviour of the system. Furthermore, Fast Fourier Transform (FFT) analysis was performed to identify and approximate the characteristic frequency of free vibrations Results are collected in Table 2. The results of the free vibraiton study are shown in Figures 5 to 9.

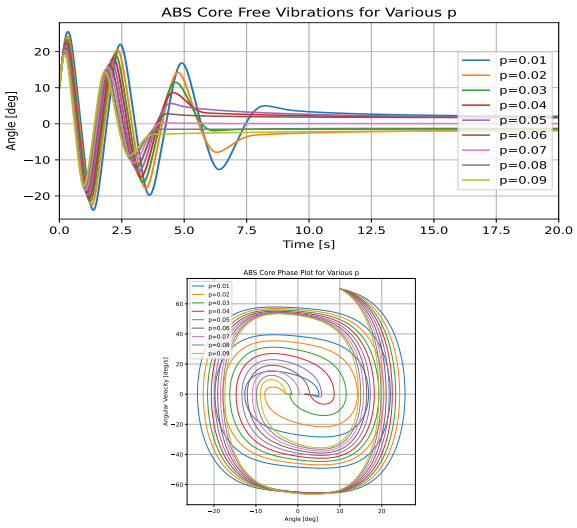

Fig. 5. Simulation results for ABS core; ICs: $\varphi_1(t) = 10$, $\dot{\varphi}_1(t) = 55$

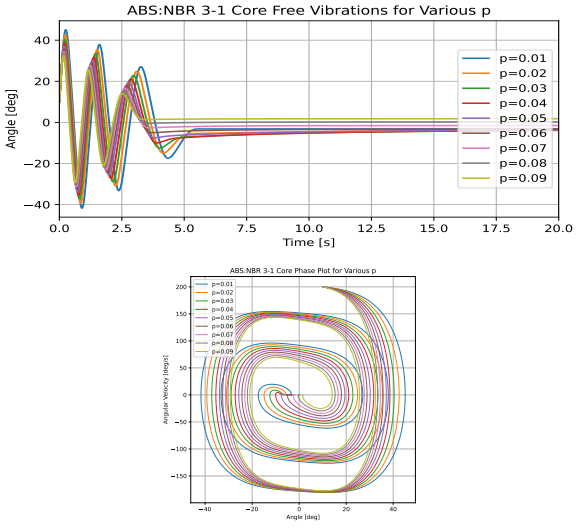

Fig. 6. Simulation results for ABS:NBR 3-1 core; ICs: $\varphi_1(t) = 10$, $\dot{\varphi}_1(t) = 160$

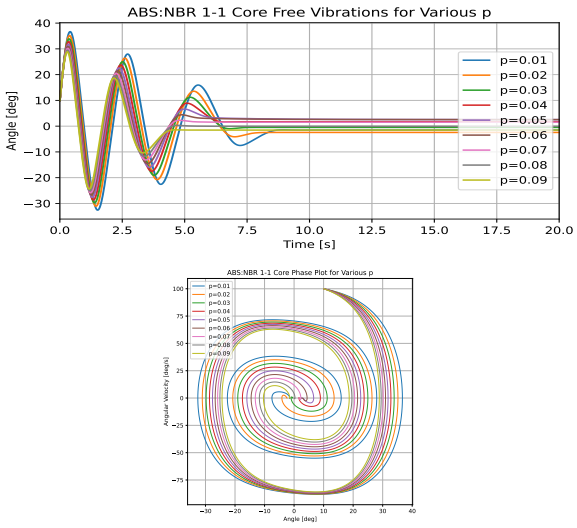

Fig. 7. Simulation results for ABS:NBR 1-1 core; ICs: $\varphi_1(t) = 10$, $\dot{\varphi}_1(t) = 100$

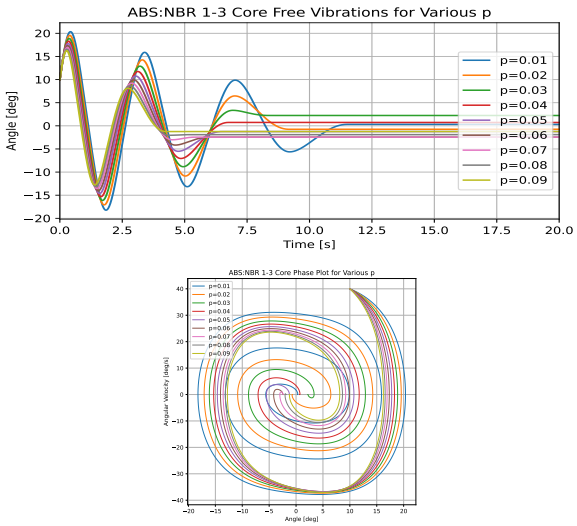

Fig. 8. Simulation results for ABS:NBR 1-3 core; ICs: $\varphi_1(t) = 10$, $\dot{\varphi}_1(t) = 40$

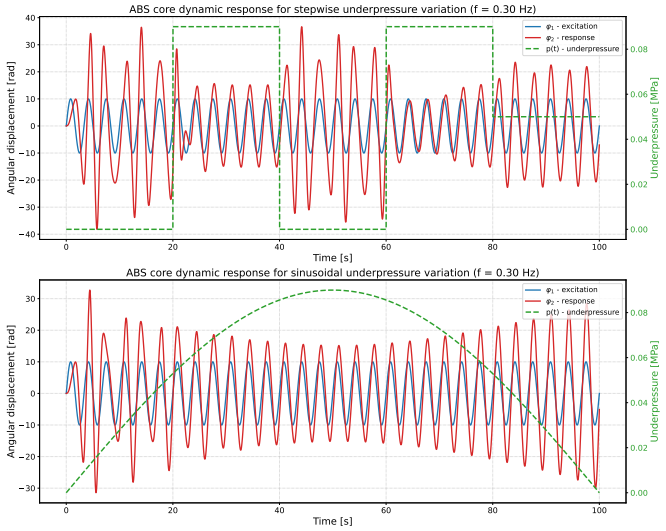

Fig. 10. ABS core time response for variable underpressure levels.

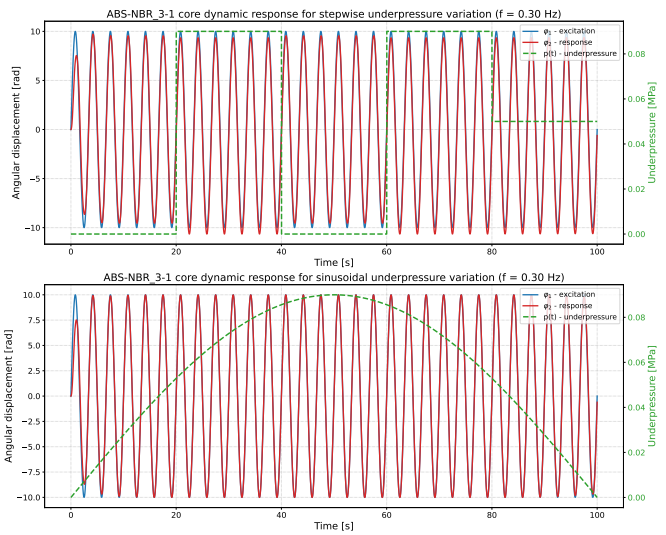

Fig. 11. ABS:NBR (3:1) core time response for variable underpressure levels.

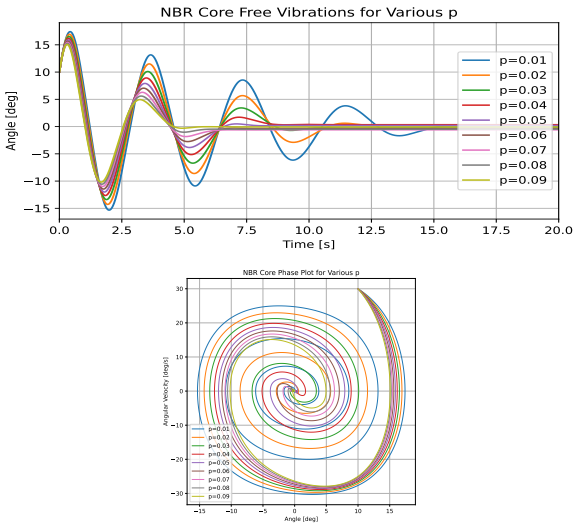

Fig. 9. Simulation results for NBR core; ICs: $\varphi_1(t) = 10$, $\dot{\varphi}_1(t) = 5$

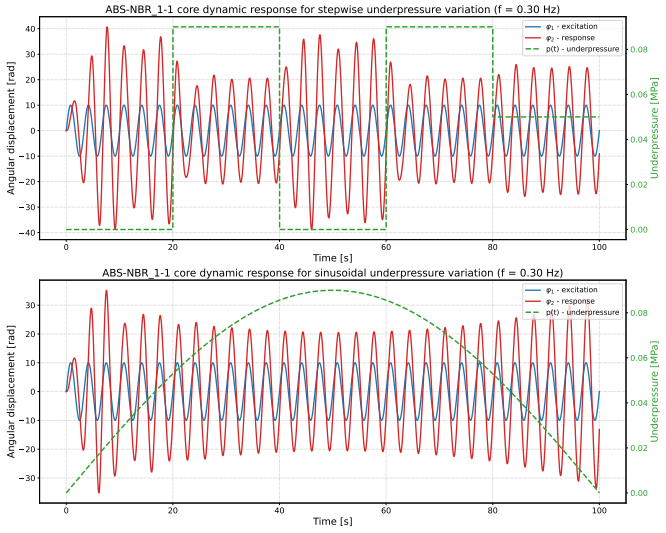

Fig. 12. ABS:NBR (1:1) core time response for variable underpressure levels.

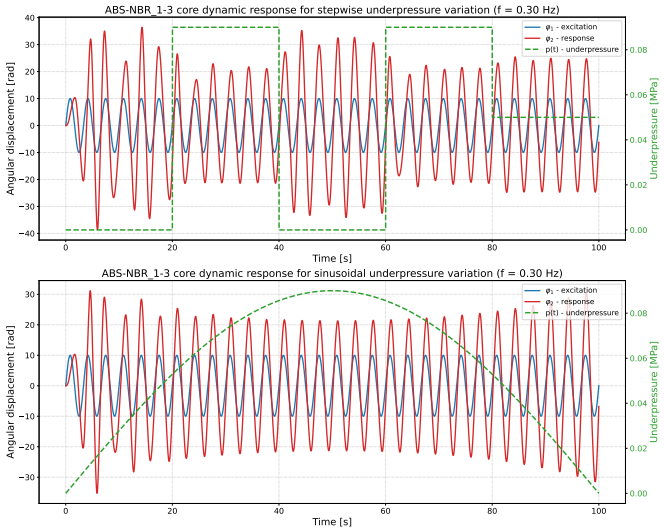

Fig. 13. ABS:NBR (1:3) time response for variable underpressure levels.

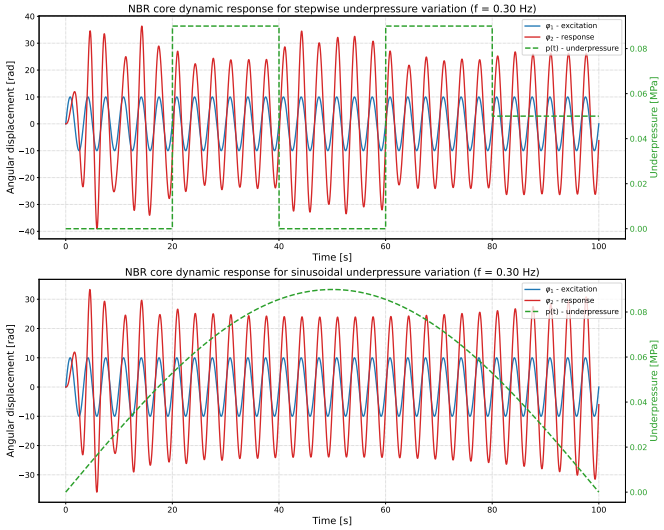

Fig. 14. NBR core time response for variable underpressure levels.

5. RESULTS AND DISCUSSION

5.1. Free vibrations

The Bouc–Wen model is difficult to identify because many different combinations of parameters can produce very similar responses. In addition, even a small change in one of the parameters may lead to significant differences in the predicted response or may even prevent the computation from converging. Furthermore, the basic Bouc–Wen model has known limitations when describing materials exhibiting hardening behaviour [21, 22, 23].

In contrast, the proposed modified Bouc-Wen model demonstrates stable behaviour across the entire range of underpressures and excitation frequencies tested. The model remains robust even when relatively large initial conditions are applied, with no issues related to numerical divergence.

The damping behaviour observed in the free vibration simulations can generally be classified as underdamped, as evidenced by the presence of oscillatory decay. However, the response is strongly dependent on the magnitude of the initial conditions. For smaller initial displacements and velocities, materials based on pure ABS or ABS:NBR mixtures exhibit a tendency to decay before crossing zero displacement. This may indicate a shift toward critically damped or even overdamped behaviour under low initial energy conditions.

In general, the damping can be considered relatively high. For all material configurations, the system converges to a steady-state displacement after oscillations decay. Interestingly, depending on the underpressure, the final static displacement can settle either slightly below or above the original zero angle position. This effect is particularly prominent for pure ABS, where the dry friction component is dominant. For each material, there exists a specific underpressure at which the system converges to a position very close to zero. As the proportion of ABS in the mixture decreases, the final equilibrium

Table 2. Characteristic frequencies of free vibration for different material mixtures at nominal underpressure.

Material Mixture	Natural Frequency [Hz]
ABS	0.35–0.52
3:1 (ABS:NBR)	0.55–0.75
1:1 (ABS:NBR)	0.37–0.5
1:3 (ABS:NBR)	0.28–0.38
NBR	0.25–0.3

tends to align more closely with the zero position.

In mixtures containing ABS, the system often oscillates around a shifted equilibrium position. This shift is a direct consequence of dry friction effects and depends on the history of the motion and initial conditions. There is a potential to predict the direction of this shift - whether it will occur above or below the original zero position - but this aspect requires further investigation and will be addressed in future studies.

As the underpressure increases, the characteristic frequency of free vibration of the system also increases. This trend is consistent across all material configurations. The presence of NBR lowers the characteristic frequencies, while the presence of ABS increases them. However, pure ABS does not exhibit the highest characteristic frequency. The highest frequency is observed for ABS:NBR 3-1, and the lowest for pure NBR. Based on the identified model parameters (summarised in Table 1) and an assumed moment of inertia $I = 0.51kg \cdot m^2$ (calculated from the real damper geometry), the estimated characteristic frequencies of free vibration are collected and shown in Table 2.

5.2. Forced vibrations

Figures 10 to 14 illustrate the response of the system to a variable underpressure level applied to the damper. The plots show the angular displacements of the excitation and damper, as well as the corresponding amplitudes of excitation and damping under slowly varying pressure conditions. In the first case, the pressure changes within 20 ms, which corresponds to the experimental tests. In the second case, the pressure varies from 0 to 0.09 MPa according to a sinusoidal function that completes half a period during the entire simulation. All simulations were performed at a frequency of excitation equal to 0.3 Hz. The analysis focused only on steady-state vibrations, neglecting the initial stage of motion when the system starts from the point (0,0).

In the case of ABS (Fig. 10), ABS-NBR 1-1 (Fig. 12), ABS-NBR 1-3 (Fig. 13), and NBR (Fig. 14), the application of vacuum results in a rapid reduction in the vibration amplitude of the damper. The increase in stiffness and damping couples the two degrees of freedom, preventing the system from entering a counter-phase oscillation mode. When analysing ABS, ABS-NBR 1-1, ABS-NBR 1-3 and NBR, it can be observed that during the final stage of the simulation, when the pressure decreases to 0.05 MPa, the response amplitude increases proportionally with the pressure drop. Slow variations in pressure also show that the response amplitude is proportional to the level of underpressure and can be precisely controlled.

For the ABS-NBR 3-1 mixture 11, regardless of the applied vacuum level, the system remains strongly coupled. As a result, the amplitude differences between the two oscillating components are negligible. This behaviour can be attributed to the highest damping capacity among all tested materials. The same behaviour can be observed in the case of slow variations of the pressure.

The clear and immediate effect of the underpressure on the system's dynamic response indicates the potential for effective use of VPPTD in active or semi-active vibration control applications.

In summary, the proposed modified Bouc-Wen model provides a reliable framework for simulating the dynamic behaviour of VPPTDs over a broad operational range. However, further research is necessary to fully characterise non-linear resonance phenomena and develop more accurate predictive tools for engineering applications.

5.3. Model limitations

Despite the good performance of the modified Bouc–Wen model, several limitations of the present study should be acknowledged.

First, the model parameters were identified from quasi-static experiments. Although this approach captures the main hysteretic behaviour of the damper, it does not fully account for possible rate-dependent effects, such as velocity-dependent stiffness or inertia effects within the granular medium.

Second, the frequency response analysis is based on steady-state amplitudes obtained after the transient response decays. As a result, certain nonlinear phenomena, such as jump resonance, multistability, or bifurcations, may not be fully captured.

Third, the current model assumes simplified excitation and does not include structural interactions that may occur when the damper is integrated into larger mechanical systems.

Finally, this study focuses only on ABS–NBR particle mixtures. Other materials, particle geometries, or size distributions can lead to different contact conditions and friction behaviour, potentially altering the dynamic response of vacuum-packed particle dampers.

6. CONCLUSION

This study presented a modified Bouc–Wen model for the dynamic simulation of Vacuum Packed Particles Torsional Dampers (VPPTDs) using mixtures of ABS and NBR particles. The proposed formulation improves numerical stability compared to the classical Bouc–Wen model and enables reliable simulations over a wide range of underpressures and excitation conditions.

The results show that the dynamic behaviour of the damper is strongly dependent on both the vacuum level and the composition of the particle mixture. Increasing underpressure leads to higher stiffness and natural frequencies, while the proportion of ABS and NBR particles influences both the damping capacity and the equilibrium position shift associated with dry friction.

The simulations clearly demonstrate that the vibration amplitude of the system can be effectively controlled by adjusting the level of underpressure in the damper. This property highlights the potential of VPPTDs for adaptive and semi-active vibration control applications.

Overall, the simulations confirm that vacuum-packed particle dampers can effectively reduce vibration amplitudes and that the proposed model provides a useful framework for analysing their dynamic behaviour.

Future work will focus on incorporating rate-dependent effects, analysing nonlinear resonance phenomena in more detail, and validating the model experimentally for broader excitation conditions and particle materials. In addition, alternative modelling approaches that could replace the modified Bouc–Wen formulation will be investigated, including models proposed in the literature [24, 25, 26, 23].

ACKNOWLEDGEMENTS

The research was funded by Warsaw University of Technology within the Excellence Initiative: Research University (IDUB) programme

REFERENCES

[1] M. Żurawski, C. Graczykowski, and R. Zalewski, "The prototype, mathematical model, sensitivity analysis and preliminary control strategy for adaptive tuned particle impact damper," *Journal of Sound and Vibration*, vol. 564, 2023.

[2] M. Żurawski and R. Zalewski, "Damping of beam vibrations using tuned particles impact damper," *Applied Sciences*, vol. 10, no. 18, 2020.

[3] S. Diao, X. Zhao, D. Zhao, Z. Dong, and Y. Qin, "Active suspension hierarchical control with parameter uncertainty and external disturbance of electro-hydraulic actuators," *Applied Mathematical Modelling*, vol. 134, pp. 50–70, 10 2024.

[4] Y. Wang, L. Li, D. Hofmann, J. E. Andrade, and C. Daraio, "Structured fabrics with tunable mechanical properties," *Nature*, vol. 596, no. 7871, pp. 238–243, Aug. 2021, (Accessed 2026-03-13).

[5] P. Gardonio, E. Rustighi, S. Baldini, C. Malacarne, and M. Perini, "In-vacuo adaptive beam element for vibration control," *Mechanical Systems and Signal Processing*, vol. 224, p. 112089, 2025.

[6] E. Rustighi, P. Gardonio, S. Baldini, C. Malacarne, and M. Perini, "Vibration response of in-vacuo tuneable structured fabrics," *Journal of Vibration and Control*, vol. 31, no. 1-2, pp. 4–23, 2025.

[7] M. Żurawski and R. Zalewski, "Experimental studies on adaptive-passive symmetrical granular damper operation," *Materials*, vol. 15, no. 17, 2022.

[8] D. Rodak, M. Żurawski, M. Gmitrzuk, and L. Starczewski, "Possibilities of vacuum packed particles application in blast mitigation seats in military armored vehicles," *Bulletin of the Polish Academy of Sciences Technical Sciences*, vol. 70, no. 1, 2022.

[9] J. D. Brigido, S. G. Burrow, B. K. Woods, P. Bartkowski, and R. Zalewski, "Flexural models for vacuum-packed particles as a variable-stiffness mechanism in smart structures," *Phys. Rev. Appl.*, vol. 17, p. 044018, Apr 2022.

[10] A. Mackojc, B. Chiliński, and R. Zalewski, "Preliminary research of a symmetrical controllable granular damper prototype," *Bulletin of the Polish Academy of Sciences Technical Sciences*, vol. 70, no. 3, 2022.

[11] R. Zalewski, P. Chodkiewicz, and M. Shillor, "Vibrations of a mass-spring system using a granular-material damper," *Applied Mathematical Modelling*, vol. 40, no. 17, pp. 8033–8047, 2016.

[12] D. Rodak, M. Żurawski, M. Pyrz, and R. Zalewski, "Modelling and identification of hysteresis of vacuum packed particles torsional damper," *Journal of Sound and Vibration*, vol. 616, p. 119203, 2025.

[13] D. Rodak and R. Zalewski, "Innovative controllable torsional damper based on vacuum packed particles," *Materials*, vol. 13, no. 19, 2020.

[14] I. D. Mayergoyz, "Vector preisach models of hysteresis," *The Science of Hysteresis*, vol. 1-3, pp. 447–528, 1 2006.

[15] R. Bouc, "Modele mathematique d' hysteresis," *Acustica*, vol. 24, pp. 16–25, 1971.

[16] J. Y. Yoon and D. L. Trumper, "Friction modeling, identification, and compensation based on friction hysteresis and dahl resonance," *Mechatronics*, vol. 24, pp. 734–741, 9 2014. [Online]. Available: https://www.sciencedirect.com/science/article/pii/S0957415814000348#b0045

[17] P. R. Dahl, "Solid friction damping of mechanical vibrations," *AIAA Journal*, vol. 14, pp. 1675–1682, 1976.

[18] F. Ikhouane, V. Mañosa, and G. Pujol, "Minor loops of the dahl and lugre models," *Applied Mathematical Modelling*, vol. 77, pp. 1679–1690, 1 2020.

[19] N. Vaiana and L. Rosati, "Analytical and differential reformulations of the vaiana–rosati model for complex rate-independent mechanical hysteresis phenomena," *Mechanical Systems and Signal Processing*, vol. 199, p. 110448, 9 2023.

[20] F. Ikhouane and J. Rodellar, *Systems with Hysteresis*. John Wiley & Sons, Inc., 2007.

[21] P. Bartkowski, R. Zalewski, and P. Chodkiewicz, "Parameter identification of bouc-wen model for vacuum packed particles based on genetic algorithm," *Archives of Civil and Mechanical Engineering*, vol. 19, pp. 322–333, 3 2019.

[22] M. Lin, B. Sun, C. Cheng, B. Zhao, Z. Peng, and G. Meng, "Alternating state-parameter identification of bouc-wen hysteretic systems from steady-state harmonic response," *Journal of Sound and Vibration*, vol. 538, p. 117242, 2022.

[23] N. Vaiana and L. Rosati, "Extended classification and generalized Vaiana–Rosati model accounting for rate-independent hysteresis loops with evolving shape," *Mechanical Systems and Signal Processing*, vol. 242, p. 113606, 2026.

[24] R. Capuano, N. Vaiana, and L. Rosati, "Frequency-response curves for rate-independent hysteretic mechan-

ical responses of complex shape," *Nonlinear Dynamics*, vol. 112, no. 7, pp. 5151–5175, Apr. 2024.

[25] R. Capuano, N. Vaiana, and L. Rosati, "MDoF mechanical systems with rate-independent hysteresis: Assessment of dimensionality, loop shapes, and mass ratio," *Chaos, Solitons & Fractals*, vol. 200, p. 117062, 2025.

[26] N. Vaiana and L. Rosati, "Classification and unified phenomenological modeling of complex uniaxial rate-independent hysteretic responses," *Mechanical Systems and Signal Processing*, vol. 182, p. 109539, 2023.